RE-ENTRANT JET MODELLING FOR PARTIALLY CAVITATING TWO-DIMENSIONAL HYDROFOILS

P. Krishnaswamy and P. Andersen
Technical University of Denmark

S.A. Kinnas,
University of Texas at Austin

Abstract

The computational analysis of partial sheet hydrofoil cavitation in two dimensions is performed. Particular attention is given to the method of simulating the flow at the end of the cavity. A fixed-length partially cavitating panel method is used to predict the height of the re-entrant jet, using the values of the cavitation number and the drag coefficient. The jet surface is subsequently constructed and included in an updated cavity shape. A source singularity is introduced in the fluid domain to account for the mass flux through the part of the domain boundary represented by the re-entrant jet surface. Further iterations are performed for fixed cavitation number on the cavity with a re-entrant jet cavity termination model. This model is seen to produce good results and displays quick convergence. A validation is accomplished by conducting a parametric analysis of the model and comparing the present calculations with other numerical schemes. The flow around the partially cavitating hydrofoil with a re-entrant jet has also been treated with a viscous/inviscid interactive method with favourable results.

1 Introduction

The present work addresses the computational analysis of partially cavitating flow for two-dimensional hydrofoils. For the nonlinear analysis of the flow around partially and supercavitating two-dimensional hydrofoils Kinnas & Fine (1990) developed a potential-based boundary element method (BEM). They found that when the method was applied to partially cavitating hydrofoils (for given cavity length and cavitation number unknown), the solution converged to the final cavity shape with fewer iterations than previously developed velocity-based BEMs (Uhlman Jr, 1987). In the current analysis, particular attention is given to the method of simulating the flow at the end of the cavity which is a highly turbulent zone characterized by two-phase flow, unsteadiness and instabilities. Most cavity closure models have been formulated to comply with the theoretical analysis of the cavitating flow problem while at the same time attempting to model the physical reality. Kinnas & Fine (1990, 1993b) described the use of a *pressure recovery termination* model. By this, a simple algebraic expression of the pressure recovery is empirically enforced over a prescribed range of the cavity length at the end of the cavity. This approach may however influence the final results.

In real flow a re-entrant jet will occur. The formation of the jet influences the shedding of cloud cavitation and subsequent generation of noise by its implosion. It also influences the volume of the cavity. The formation of a re-entrant jet cavity produced in symmetric flow against a vertical flat plate was investigated by Birkhoff (1948) and Gilbarg (1960). Simple relations between the relative cavity cross-section and the drag coefficient which apply to any symmetrical obstacle in the plane and to any axially symmetric obstacle in space were derived by Birkhoff (1948).

Dang & Kuiper (1998) presented a potential-based panel method that predicts the partial cavity flow on two-dimensional hydrofoil sections using a re-entrant jet model. The cavity shape and extent were determined for given cavitation number and the re-entrant jet surface was formed automatically as the cavity became fully developed.

The aim of the present work is to outline an alternative formulation of the re-entrant jet cavity closure model and its numerical implementation in conjunction with the fixed-length boundary element method,

PCPAN (Partially Cavitating PANel method) (Kinnas & Fine, 1993a). The intention is to exploit the quick convergence and the good cavity prediction properties of PCPAN to make an accurate prediction of the height of the re-entrant jet and construct a good initial guess for the re-entrant jet solution. The following key points are then addressed:

- Computation of the theoretical height of the re-entrant jet.
- Parametric analysis of the numerical implementation of the re-entrant jet model.
- Investigation of the robustness and the limitations of the re-entrant jet model.

The analysis of the re-entrant jet model is taken one step further by including viscous effects. This is done by coupling the potential flow solution to a boundary layer solver (Brewer, 1995, 1996) which has been suitably modified to take into account the presence of the re-entrant jet.

2 Re-Entrant Jet Modelling of the Partially Cavitating Flow

A partially cavitating hydrofoil with chord length $c = 1$ subject to a uniform inflow U_∞ at an angle of attack α and with ambient pressure p_∞ is considered. See Figure 1.

It is assumed that the fluid is inviscid and incompressible and that the resulting flow is irrotational. The total velocity flow field $\mathbf{q}$ can be expressed in terms of either the total potential, Φ, or the perturbation potential, ϕ, as follows

$$\mathbf{q} = \nabla\Phi = \mathbf{U}_\infty + \nabla\phi.$$

The inflow velocity potential Φ_{in} corresponds to the uniform inflow:

$$\Phi_{in}(x, y) = U_\infty(x \cos\alpha + y \sin\alpha).$$

The perturbation potential ϕ must satisfy Laplace's equation, $\nabla^2\phi = 0$, in the domain outside the hydrofoil and the cavity, while the equation to be solved is given by Green's theorem. Thus the perturbation potential, ϕ_P, at any point P on the cavity or the foil is given by

$$\pi\phi_P = \int_S \left(-\phi\frac{\partial \ln r}{\partial n} + \frac{\partial\phi}{\partial n}\ln r\right) ds - \int_W \Delta\phi_W \frac{\partial \ln r}{\partial n} ds \tag{1}$$

where r is the distance from the surface element ds, on the combined foil/cavity (including the re-entrant jet) surface S, to the point P, and $\Delta\phi_W$ is the potential jump in the wake.

2.1 Boundary Conditions

The re-entrant jet cross section is introduced as a boundary of the problem, on which surface a normal velocity into the cavity is prescribed which equals the free-stream velocity on the cavity surface, q_c, as shown in Figure 1.

For the flow situation illustrated in Figure 1, the mass flux (per unit length) through the re-entrant jet surface is equal to $\rho q_c h$, where h denotes the height of the re-entrant jet. This flux is accounted for by introducing a *source* at a specified position in the fluid domain. The strength of the source $Q = hq_c$ corresponds to the flux through the re-entrant jet surface. The dynamic boundary condition on the cavity requires the pressure to be constant on the cavity surface. Applying Bernoulli's equation and the definition of the cavitation number $\sigma = (p_\infty - p_v)/\frac{\rho}{2}U_\infty^2$, gives the magnitude of the total velocity on the cavity surface, $q_c = U_\infty\sqrt{1+\sigma}$.

Naturally, the effect of the source needs to be included in the kinematic boundary conditions on the wetted foil and cavity surface as well as the re-entrant jet surface. The normal derivative

$$\frac{\partial\phi_{\text{source}}}{\partial n} = \frac{\partial\phi_{\text{source}}}{\partial r}\left(\frac{\mathbf{n}\cdot\mathbf{r}}{|\mathbf{r}|}\right).$$

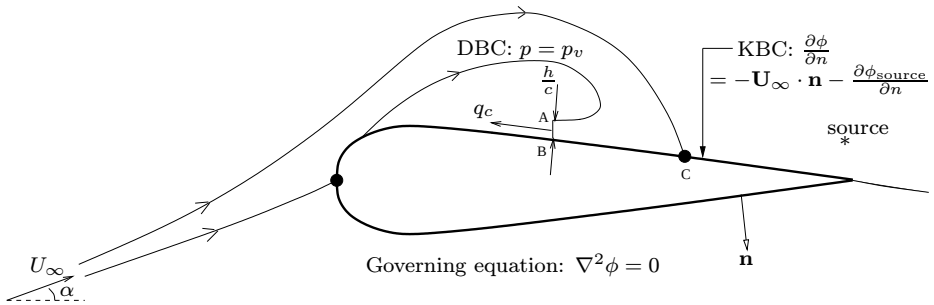

Figure 1: *Sketch of a cavitating 2D blade with a re-entrant jet. The thick curve denotes the foil surface. The source singularity is placed close to the blade trailing edge.*

By use of the expression for the source strength $Q = hU_\infty\sqrt{1+\sigma}$, the following kinematic boundary conditions are obtained

$$\frac{\partial\phi}{\partial n} = -\mathbf{U}_\infty \cdot \mathbf{n} - \frac{U_\infty h\sqrt{1+\sigma}}{2\pi r}\left(\frac{\mathbf{n}\cdot\mathbf{r}}{|\mathbf{r}|}\right) \text{ on the wetted foil and cavity surface,} \tag{2}$$

$$\frac{\partial\phi}{\partial n} = -\mathbf{U}_\infty \cdot \mathbf{n} - U_\infty\sqrt{1+\sigma}\left(1 + \frac{h}{2\pi r}\left(\frac{\mathbf{n}\cdot\mathbf{r}}{|\mathbf{r}|}\right)\right) \text{ on the jet surface.} \tag{3}$$

Furthermore, a Kutta condition prescribing $\nabla\phi$ to be finite at the trailing edge is applied, and finally a condition requiring $\nabla\phi \to 0$ is imposed.

2.2 Computing the Height of the Re-Entrant Jet

The theoretical height of the re-entrant jet is calculated by applying the continuity and momentum balance equations on a control volume of the fluid shown by the shaded region in Figure 2. In the shown configuration, it is assumed that the thickness of the jet is constant after having entered the cavity at an angle β with respect to the x-axis. Furthermore, the pressure forces acting on the physical boundary of the control volume are ignored.

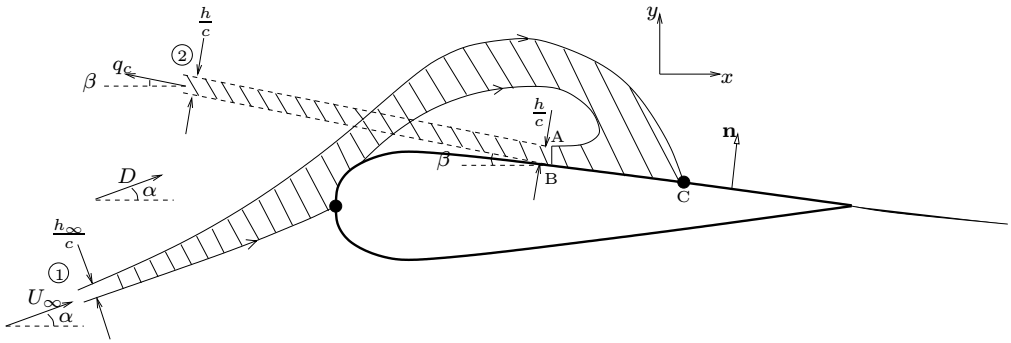

Figure 2: *The control volume for the continuity and momentum balance equations.*

The continuity equation leads to the following relation:

$$\frac{h}{h_\infty} = \frac{U_\infty}{q_c}. \tag{4}$$

The momentum equation in the x-direction yields

$$D\cos(\alpha) = -\rho U_\infty^2 h_\infty \cos(\alpha) - \rho q_c^2 h \cos(\beta). \tag{5}$$

Combining (4) and (5) yields the following expression for the non-dimensionalized height of the re-entrant jet:

$$\frac{h}{c} = \frac{C_D \cos(\alpha)}{2[\sqrt{1+\sigma}\cos(\alpha) + (1+\sigma)\cos(\beta)]}, \tag{6}$$

where the negative sign that would otherwise purely indicate the direction of the flow velocity vector at the re-entrant jet section, has been ignored and the drag coefficient, $C_D = D/\left(\frac{1}{2}\rho U_\infty^2 c\right)$.

For $\alpha = \beta = 0$

$$\frac{h}{c} = \frac{C_D}{2(\sqrt{1+\sigma} + 1 + \sigma)},$$

which is the thickness as derived by Birkhoff (1948) of the re-entrant jet formed by the symmetric flow past an obstacle.

3 Numerical Implementation of the Re-Entrant Jet Model

Based on a converged solution found for fixed cavity-length using PCPAN (Kinnas & Fine, 1993a), the height of the re-entrant jet, h/c, is computed using the converged values of the drag coefficient, C_D, and the cavitation number, σ, in accordance with (6). The cavity shape is then updated, firstly by erecting the jet surface with length h/c normal to the foil, at the point where the cavity calculated in PCPAN re-attaches to the foil, and subsequently increasing the cavity thickness distribution linearly from the detachment point to the jet. This is an initial guess for subsequent iterations for fixed cavitation number and fixed position of the jet, $x_{\rm jet}/c$. The calculation of the height of the jet and the construction of the initial guess of the cavity shape are performed in a subroutine **jetht** while the iterative procedure for the cavity shape with the re-entrant jet is carried out in a subroutine **pcjet**. Both subroutines, **jetht** and **pcjet**, work in conjunction with PCPAN. A sample case for a NACA 16-006 section with zero camber is shown in Figure 3.

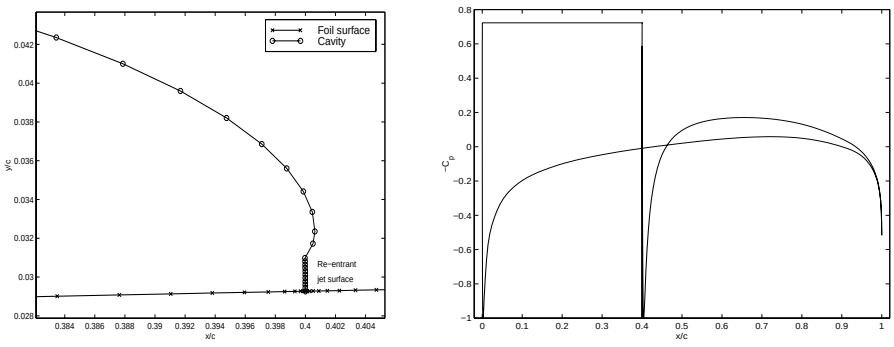

(a) Cavity closure region (b) Pressure distribution

Figure 3: *Converged solution after 18 iterations for a NACA 16-006 section at* $\alpha = 3°$, $\sigma = 0.72271$, $h/c = 0.00171$, $l/c = 0.40063$, $V/c^2 = 0.00758$, $C_L = 0.37546$, $C_D = 0.00947$.

Figure 4 shows the solution after another seven iterations for which the jet surface is moved upstream such that $x_{\rm jet}/c = 0.392$. The more pronounced re-entrant jet structure leads to a slight increase in the cavity volume. It should be noted that the cavity shown in Figure 4 does not represent a converged solution. The pressure distribution in Figure 4 clearly shows the stagnation point ($-C_p = -1$) abaft the end of the cavity. The location of this point is indicated by the letter C in the Figures 1, 2 and 4.

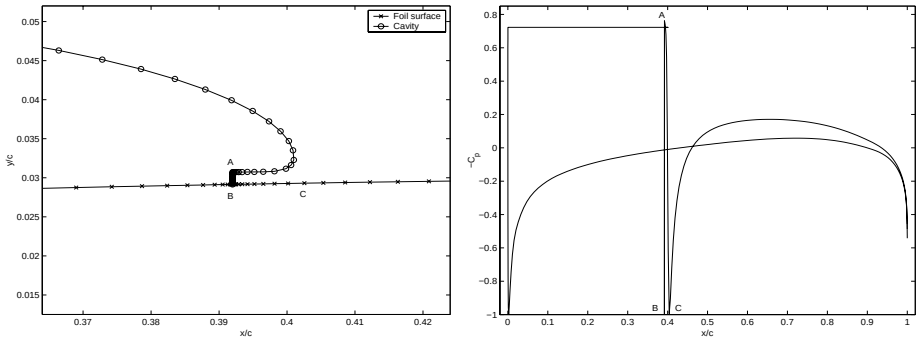

(a) Cavity closure region (b) Pressure distribution

Figure 4: *NACA 16-006 at* $\alpha = 3°$*, for* $\sigma = 0.72271$*,* $x_{jet}/c = 0.392$*,* $V/c^2 = 0.00763$*,* $C_L = 0.37403$*,* $C_D = 0.00946$ *and* $l/c = 0.40099$

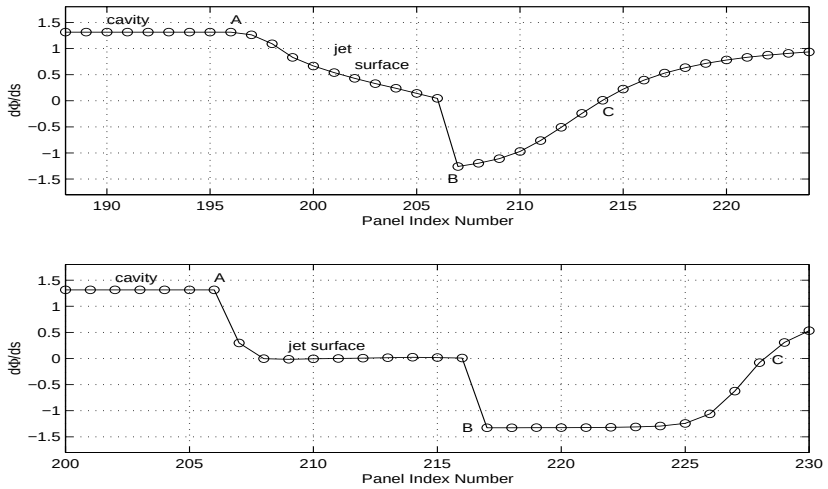

Figure 5: *Velocity profiles for the NACA 16-006 section at* $\alpha = 3°$ *and* $\sigma = 0.72271$*; converged solution for* $x_{jet}/c = 0.4$ *(top); solution after jet is moved to 0.392*

The moving of the jet surface also has a positive influence on the distribution of the total velocity, $\partial\Phi/\partial s$, as is shown in Figure 5. The top figure shows the velocity distribution of the cavity closure region corresponding to the converged solution shown in Figure 3 where $x_{\rm jet}/c = 0.4$. As expected the velocity along the cavity surface equals $q_c = \sqrt{1+\sigma} = \sqrt{1+0.72271} = 1.3125$. In this case where the re-entrant jet behaviour is not so pronounced, the jet panels have a small tangential velocity component that gradually approaches zero as the jet re-attaches to the foil. However in the case where the jet surface is moved upstream such that $x_{\rm jet}/c = 0.392$, the tangential velocity components of nearly all the jet panels are close to zero in accordance with the physical model which prescribes a normal velocity (now almost parallel to the foil surface) into the cavity equal to the free-stream velocity on the cavity surface, q_c. The points A and B on the two figures correspond to the point where the cavity attaches to the jet surface and the point where the jet attaches to the foil respectively. The locations of these points are also marked in the Figures 1, 2 and 4.

4 Validating the Implemented Re-Entrant Jet Model

In analogy to the numerical results presented by Dang & Kuiper (1998), a parametric analysis is performed by a series of calculations for NACA 16 series sections with different thickness to chord ratio and zero camber.

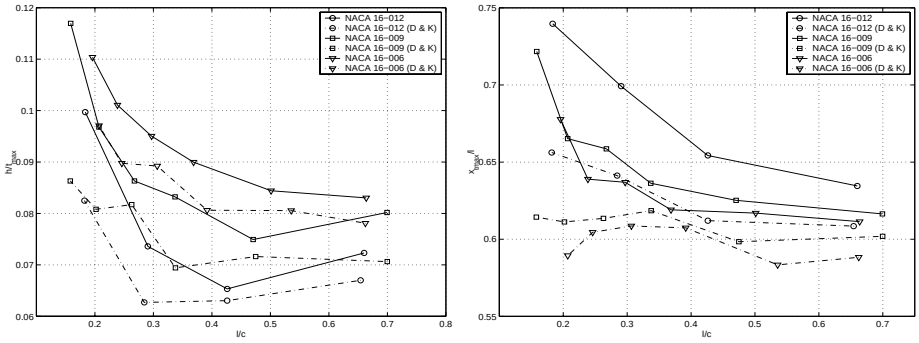

(a) $h/t_{\max}$ vs. l/c (b) x_{tmax}/l vs. l/c

Figure 6: *Comparisons with results obtained by Dang & Kuiper (1998) for the jet and the cavity thickness.*

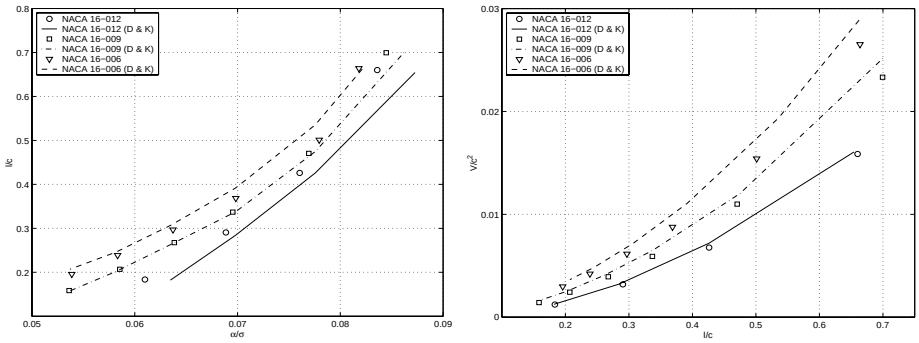

(a) l/c vs. α/σ (b) V/c^2 vs. l/c

Figure 7: *Comparisons with results obtained by Dang & Kuiper (1998) for the cavity shape.*

Figure 6 (left) shows that the re-entrant jet thickness is always a certain percentage (between 6 % and 12 %) of the maximum cavity thickness $t_{\max}/c$ irrespective of the cavitation number and the profile thickness. It is established that the thickness of the re-entrant jet is greater for thinner foils and vice versa. It is also seen when comparing the corresponding curves for each of the foil sections that the values of $t_{\max}/c$ found using **pcjet** are marginally smaller than their counterparts found by Dang & Kuiper (1998). In Figure 6 (right) it is seen that the maximum cavity thickness is consistently situated at a point that is approximately between 60 % and 70 % of the cavity length irrespective of the cavitation number and the profile thickness. The maximum cavity thickness is located further downstream in the solutions found using **pcjet**.

A combination of the results illustrated in Figure 6 seems to indicate that the cavity shapes calculated using **pcjet** are slightly more elongated than the corresponding cavities found by Dang & Kuiper (1998). This could be attributed to the influence of the source singularity on the cavity panels. A direct comparison of the cavity shapes would be required to establish this effect.

A comparison between the calculated cavity lengths for the two numerical methods with the re-entrant jet is shown in Figure 7 (left). It is found that the results for the NACA 16-009 section are very close to each

other. However the cavity predicted by the present method is slightly shorter for the NACA 16-006 section but longer for the NACA 16-012 section as compared to those calculated by Dang & Kuiper (1998). In accordance with the nonlinear cavitation theory, both methods predict a decrease in the cavity length with increasing foil thickness. Figure 7 (right) shows that the present method predicts a smaller cavity volume for the NACA 16-006 section and the NACA 16-009 section. However, the cavity volume results for the NACA 16-012 section are close to each other.

To further assess the difference of the cavity prediction results between the present method and other nonlinear methods, comparisons are made with calculations by Uhlman Jr (1987) in which he used a termination wall cavity closure model. Uhlman Jr (1987) used a velocity-based method in which the cavitation number is calculated for a prescribed cavity length. Once again, the calculations are performed on NACA 16 series sections at an angle of attack, $\alpha = 4^\circ$, for different cavitation numbers. The results obtained for the cavity length by Krishnaswamy (2000) showed good agreement for the NACA 16-009 section while the results for the cavity volume showed that the present method predicted slightly smaller cavities as compared to the method implemented by Uhlman Jr (1987).

The comparisons made between the present method using **pcjet** and the methods implemented by Dang & Kuiper (1998) and Uhlman Jr (1987) validate the current formulation. In particular, the results for the NACA 16-009 section coincide well for the three methods.

5 Viscous Calculations with the Re-Entrant Jet

The following addresses the issue of viscosity in partially cavitating flow. The numerical method CAV2DBL presented by Brewer (1995) finds the boundary layer on the cavity surface resulting from the fully nonlinear cavity analysis performed in PCPAN. Thus the method couples the existing inviscid flow solution to a boundary layer solver. In the present viscous study, the method employed in CAV2DBL has been slightly modified to account for the presence of the re-entrant jet and implemented on cases in unbounded flow by Krishnaswamy (2000).

The objective now is to investigate whether the inclusion of the re-entrant jet enhances the compatibility of CAV2DBL with experimental results. To this effect, a case for the NACA 66(MOD), $a = 0.8$, $t/c = 0.09$, $f/c = 0.02$ is considered in accordance with the measurements carried out by Shen & Dimotakis (1989).

	σ^v	l/c	C_L
Experimental (S & D)	0.91	0.36	0.670
Solution based on **pcjet**	0.97652	0.36024	0.63465

Table 1: *Comparing the viscous solutions found using CAV2DBL with an experimental measurement for the partially cavitating NACA 66(MOD), $a = 0.8$, $t/c = 0.09$, $f/c = 0.02$ at $\alpha = 4^\circ$ and with $Re = 2 \times 10^6$ (Shen & Dimotakis, 1989).*

The case considered in the following is for an angle of attack, $\alpha = 4^\circ$ and cavity length $l/c = 0.36$. In the experiments, this condition was achieved for the cavitation number $\sigma = 0.91$. Inviscid numerical calculations are initially performed using **pcjet**. The inviscid solution grossly overpredicts the value of the cavitation number and the lift coefficient despite the inclusion of the wall effects by the principle of images.

Using CAV2DBL to perform viscous calculations on the compound foil generated by **pcjet**, a converged solution is obtained after seven iterations. The transition points are set at 13% of the chord length on the suction side and 89% of the chord length on the pressure side.

Table 1 shows the results of the viscous calculations where the viscous cavitation number for the numerical calculations is calculated by averaging the value of $-C_p^{vis}$ over the extent of the cavity where the pressure distribution is roughly constant. Figure 8 shows that the re-entrant jet solution displays a small pressure peak close to the foil leading edge which was also evident for the viscous calculations in unbounded flow. This is attributed to the influence of the change in the direction of the flow in the cavity closure region, which influences the strength of the blowing sources used to model the boundary layer in this region (Krishnaswamy, 2000).

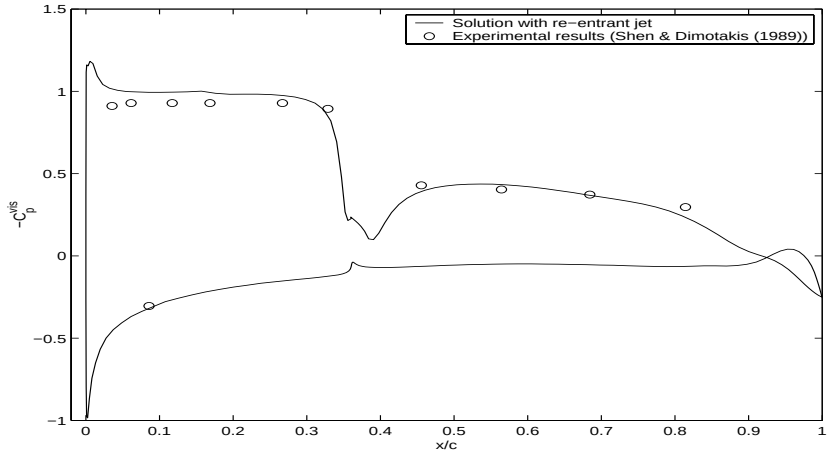

Figure 8: *Comparing the viscous pressure distribution for the viscous solutions (using CAV2DBL) with the experimental data for the partially cavitating NACA 66(MOD),* $a = 0.8$, $t/c = 0.09$, $f/c = 0.02$ *at* $\alpha = 4°$.

6 Conclusions

A potential based panel method employing a re-entrant jet cavity closure model is developed to predict the cavitation around an arbitrary partially cavitating two-dimensional foil section. A source singularity is introduced in the fluid domain to account for the mass flux through the part of the domain boundary represented by the re-entrant jet surface.

A series of calculations for NACA 16 series sections confirms the stability of the method and highlights its quick convergence. The latter is attributed to the construction of a good initial guess based on a panel method using a pressure recovery termination model. The results from these preliminary calculations are used to calculate the theoretical height of the re-entrant jet.

The implemented re-entrant jet method has been validated by a parametric analysis and by comparisons with the numerical results obtained by Dang & Kuiper (1998) and Uhlman Jr (1987). Moving the jet further upstream enhances the jet structure and has a positive effect on the total velocity distribution.

The re-entrant jet model has also been treated using a viscous/inviscid interactive method. Comparisons with experimental measurements give favourable results barring the presence of a slight pressure peak close to the foil leading edge.

Acknowledgments

This research has been financed by the Technical University of Denmark. A part of the research was carried out at the Department of Civil Engineering, University of Texas at Austin. Funding for this placement was provided by The Danish Vetlesen Fellowships for Danish Naval Architects and the Civ.ing. Kristian Rasmussen and Gunild Katrine Rasmussen Fund.

References

Birkhoff, G., Remarks on Streamlines of Discontinuity, *Revista de Ciencias, Lima*, 50:pp.105–116, 1948.

Brewer, W., *A Computational and Experimental Study of Viscous Flow Around Cavitating Propulsors*, Master's thesis, Department of Ocean Engineering, MIT, 1995.

Brewer, W., *CAV2DBL CAVitating 2 Dimensional with Boundary Layer USER'S MANUAL Version 1.0*, Department of Ocean Engineering, MIT, 1996.

Dang, J. & Kuiper, G., Re-Entrant Jet Modelling of Partial Cavity Flow on Two-Dimensional Hydrofoils, *Proceedings Third International Symposium on Cavitation, Grenoble, France, April 7-10*, 1998.

Gilbarg, D., Jets and Cavities, *Encyclopedia of Physics*, 9(3):pp.311–445, 1960.

Kinnas, S. & Fine, N., Non-Linear Analysis of Flow Around Partially or Super-Cavitating Hydrofoils by a Potential Based Panel Method, *Proceedings the IABEM-90 Symposium, University of Rome, Italy, October 15-19*, 1990.

Kinnas, S. & Fine, N., *MIT-PCPAN and MIT-SCPAN (Partially Cavitating and Super Cavitating 2-D PANel methods) User's Manual, Version 1.0*, 1993a.

Kinnas, S. & Fine, N., A numerical nonlinear analysis of the flow around two- and three-dimensional partially cavitating hydrofoils, *Journal of Fluid Mechanics*, 254:pp.151–181, 1993b.

Krishnaswamy, P., *Flow Modelling for Partially Cavitating Hydrofoils*, Ph.D. thesis, Department of Naval Architecture and Offshore Engineering, Technical University of Denmark, 2000.

Shen, Y. & Dimotakis, P., The Influence of Surface Cavitation on Hydrodynamic Forces, *Proceedings* 22^{nd} *ATTC, St. Johns*, 1989.

Uhlman Jr, J., The Surface Singularity Method Applied to Partially Cavitating Hydrofoils, *Journal of Ship Research*, 31(2):pp.107–124, 1987.